Signal Processing ∎ (∎∎∎∎) ∎∎∎–∎∎∎

Contents lists available at ScienceDirect

Signal Processing

journal homepage: www.elsevier.com/locate/sigpro

A new efficient filtered-x affine projection sign algorithm for active control of impulsive noise

Q1 Longshuai Xiao, Ming Wu, Jun Yang*

Key Laboratory of Noise and Vibration Research, Institute of Acoustics, Chinese Academy of Sciences, Beijing 100190, China

ARTICLE INFO

Article history:
Received 23 August 2015
Accepted 12 September 2015

Keywords:
Active impulsive noise control
Alpha stable distribution
Robustness
Affine projection sign algorithm
Efficient implementations

ABSTRACT

Impulsive noise is often encountered in the practical active noise control (ANC) applications. Traditional ANC algorithms fail to control such noise. Derived by minimizing the ℓ_1 norm of an estimated a posteriori error vector, a new filtered-x affine projection sign algorithm (NFxAPSA) is proposed to efficiently and effectively suppress impulsive noise. Two typical extensions, such as variable step-size design and hybrid implementation, are further adapted to strengthen the effectiveness of the new structure. Simulation results verify the superior performance of the proposed algorithm in active control of impulsive noise with both synthesized and real-world data.

1. Introduction

Based on the principle of destructive interference of propagating acoustic waves, ANC has wide applications in the cancelation of low frequency noise [1]. However, when dealing with impulsive noise, the classic ANC algorithm, such as, filtered-x least mean square (FxLMS), converges slowly or even diverges [2–9]. Many practical acoustical signals are impulsive-like, such as noise generated by stamping machines in industrial manufacturing plants, or by life-saving equipments in hospitals [10], which can be more accurately modeled by alpha stable distribution than Gaussian one [11]. The characteristic function of the standard symmetric alpha stable (SαS) distribution is $\phi(t) = \exp(-|t|^{\alpha})$ where the shape parameter α $(0<\alpha<2)$ is called the characteristic exponent [12]. A smaller α indicates the heavier tail of the density function. As is well known that, for the non-Gaussian stable distribution $(\alpha<2)$, the second-order moment is infinite. Therefore, algorithms based on the second order moment, such as FxLMS, are severely degraded by impulsive inputs.

The state-of-the-art active impulsive noise control (AINC) algorithms can be classified into four types: (i) minimization of lower order moment of error signal, either fractional lower order moment (FLOM) [2,4–6] or logarithm moment [7]; (ii) modification of abnormal input samples and/or error signal to update weight [3,4]; (iii) modified normalization of the gradient of the weight update using both the energy of input vector and error signal [5,6,8]; (iv) minimization of an M-estimate of error signal [8]. These methods either need *a priori* knowledge of α or are sensitive to threshold parameters. Furthermore, with the increase of heaviness of impulsive noise, all of these methods degrade severely, especially when $\alpha \le 1$.

The ℓ_1 norm has been known as a robust alternative to the ℓ_2 norm when used as a cost function [13,14]. Derived by minimizing ℓ_1 norm of the a posteriori error vector, the affine projection sign algorithm (APSA) is robust against impulsive interferences [15]. Modified filtered-x structure of APSA (MFxAPSA) has been shown to cancel impulsive noise sources effectively [16–18]. Though efficient implementations via techniques from [19–22] can remarkably reduce computational cost of MFxAPSA, the number of multiplications of computing error vector is still too high when compared to FxLMS. By utilizing the small step-size assumptions of regular ANC algorithms, we propose a new

* Corresponding author.
E-mail address: jyang@mail.ioa.ac.cn (J. Yang).

http://dx.doi.org/10.1016/j.sigpro.2015.09.015
0165-1684/

structure of FxAPSA (NFxAPSA), which is as efficient as conventional structure [23], however, has much better performance than it. Variable step-size (VSS) design and hybrid implementation are further extended to illustrate the effectiveness of NFxAPSA.

In Section 2 we list the original MFxAPSA. The proposed NFxAPSA is derived in Section 3, next to which the VSS and hybrid extensions are also described. In the subsequent section, the complexity is analyzed. Simulation results are presented in Section 6. Finally, in the last section, we come to our conclusions.

2. The MFxAPSA

In the ANC applications, the desired signal $d(n)$ is unaccessible directly, but can be estimated as $\hat{d}(n)$ by adding the estimated canceling signal $\hat{y}_f(n)$ to the error signal $e(n)$. Then, by minimizing the ℓ_1 norm of the estimated a posteriori error vector $\hat{\mathbf{e}}_p(n)=\hat{\mathbf{d}}(n)-\mathbf{X}_f^T(n)\mathbf{w}(n+1)$, we get an optimization model for the MFxAPSA as

$$\min_{\mathbf{w}(n+1)} \quad \|\hat{\mathbf{e}}_p(n)\|_1$$
$$\text{s.t.} \quad \|\mathbf{w}(n+1)-\mathbf{w}(n)\|_2^2 \le \mu^2. \tag{1}$$

Solving the model [15], we get the weight update equation of the MFxAPSA

$$\mathbf{w}(n+1)=\mathbf{w}(n)+\mu\mathbf{x}_e(n)/\sqrt{\|\mathbf{x}_e(n)\|_2^2+\epsilon}, \tag{2}$$

where $\mathbf{x}_e(n)=\mathbf{X}_f(n)\mathrm{sgn}(\hat{\mathbf{e}}_a(n))$, $\hat{\mathbf{e}}_a(n)=\hat{\mathbf{d}}(n)-\mathbf{X}_f^T(n)\mathbf{w}(n)$, $x_f(n)=\hat{\mathbf{s}}^T\mathbf{x}_{\hat{M}}(n)$, and $y(n)=\mathbf{x}^T(n)\mathbf{w}(n)$. The related quantities are defined as $\mathbf{X}_f(n)=[\mathbf{x}_f(n),\mathbf{x}_f(n-1),\ldots,\mathbf{x}_f(n-P+1)]$, $\mathbf{x}_f(n)=[x_f(n),x_f(n-1),\ldots,x_f(n-L+1)]^T$, $\mathbf{x}_{\hat{M}}(n)=[x(n),x(n-1),\ldots,x(n-\hat{M}+1)]^T$, $\mathbf{x}(n)=[x(n),x(n-1),\ldots,x(n-L+1)]^T$, $\hat{\mathbf{d}}(n)=[\hat{d}(n),\hat{d}(n-1),\ldots,\hat{d}(n-P+1)]^T$, $\mathbf{y}_M(n)=[y(n),y(n-1),\ldots,y(n-M+1)]^T$, $\mathbf{y}_{\hat{M}}(n)=[y(n),y(n-1),\ldots,y(n-\hat{M}+1)]^T$, $\hat{d}(n)=e(n)+\hat{\mathbf{s}}^T\mathbf{y}_{\hat{M}}(n)$, where, $e(n)=d(n)-\mathbf{s}^T\mathbf{y}_M(n)$ is the error signal in the error sensor, $\hat{\mathbf{e}}_a(n)$ is the estimated a priori error vector, $\mathbf{s}$ and $\hat{\mathbf{s}}$ are the true and estimated secondary paths, $L,P,M,\hat{M}$ are the filter, projection, true and estimated secondary path length, respectively, μ,ϵ are step-size and regularization parameters, T represents transposition operation, $\mathrm{sgn}(\cdot)$ is a sign function.

3. The proposed NFxAPSA

The direct computation of $\hat{\mathbf{e}}_a(n)$ requires PL multiplications, which may limit the projection order to be small for realtime applications. Motivated by Ni's exact efficient implementation of the APSA [19], we recursively compute $\hat{\mathbf{e}}_a(n)$ via utilizing the shift structure of inputs. Rewrite the weight update equation of the MFxAPSA as

$$\mathbf{w}(n+1)=\mathbf{w}(n)+\mu(n)\mathbf{X}_f(n)\mathrm{sgn}(\hat{\mathbf{e}}_a(n)), \tag{3}$$

where

$$\mu(n)=\mu/\sqrt{\mathrm{sgn}(\hat{\mathbf{e}}_a^T(n))\mathbf{r}_{fse}(n)+\epsilon}, \tag{4}$$

$$\mathbf{r}_{fse}(n)=\mathbf{R}_f(n)\mathrm{sgn}(\hat{\mathbf{e}}_a(n)), \tag{5}$$

$$\mathbf{R}_f(n)=\begin{bmatrix} [\mathbf{r}_f(n)]_0 & [\mathbf{r}_f^T(n)]_{1:P-1} \\ [\mathbf{r}_f(n)]_{1:P-1} & [\mathbf{R}_f(n-1)]_{0:P-2,0:P-2} \end{bmatrix}, \tag{6}$$

$$[\mathbf{r}_f(n)]_p=[\mathbf{r}_f(n-1)]_p+x_f(n)x_f(n-p)-x_f(n-L)x_f(n-p-L). \tag{7}$$

Define $\mathbf{R}_f(n)=\mathbf{X}_f^T(n)\mathbf{X}_f(n)$ and $[\mathbf{r}_f(n)]_p=\mathbf{x}_f^T(n)\mathbf{x}_f(n-p)$, $p=0,1,\ldots,P-1$. The update of $\mathbf{R}_f(n)$ only takes $2P$ multiplications, thus the weight update needs $L+1$ multiplications. Replace $\mathbf{w}(n)$ with $\mathbf{w}(n-1)$ for computing $\hat{\mathbf{e}}_a(n)$, we get

$$\hat{\mathbf{e}}_a(n)=[\hat{e}(n)\overline{\hat{\mathbf{e}}}_p^T(n-1)]^T, \tag{8}$$

where $\overline{\hat{\mathbf{e}}}_p(n-1)$ represents the first $P-1$ elements of $\hat{\mathbf{e}}_p(n-1)$, $\hat{e}(n)=\hat{d}(n)-\mathbf{x}_f^T(n)\mathbf{w}(n)$ and

$$\hat{\mathbf{e}}_p(n-1)=\hat{\mathbf{e}}_a(n-1)-\mu(n-1)\mathbf{r}_{fse}(n-1). \tag{9}$$

Eqs. (3)–(9) constitute the primary framework of the efficient implementation of the MFxAPSA. Compared with the direct implementation of MFxAPSA (MFxAPSA-D) in Section 2, the efficient one can remarkably reduce multiplications. In the efficient implementation, we can either compute $\hat{e}(n)$ as

$$\hat{e}(n)=e(n)+\hat{\mathbf{s}}^T\mathbf{y}_{\hat{M}}(n)-\mathbf{x}_f^T(n)\mathbf{w}(n). \tag{10}$$

or using method from [21], which is more efficient when L is much larger than $\hat{M}$, we omitted the details for save of space. We call these two exact efficient implementations as MFxAPSA-EEI and MFxAPSA-EEII.

Despite of the exact efficient implementations, the number of multiplications is still large compared with FxLMS. Meanwhile, we are aware of that, due to the delay of secondary path in the context of ANC, we always assume that the weight changes little in the intervals of the secondary path length, which is a reasonable assumption for sufficiently small step-size [1,23–25]. Thus it is possible to utilize this regular assumption to further reduce the complexity of MFxAPSA-EEI. To make this clear, we expand the expression in Eq. (10) as

$$\hat{e}(n)=e(n)+\hat{\mathbf{s}}^T\mathbf{z}(n), \tag{11}$$

where

$$\mathbf{z}(n)=\begin{bmatrix} 0 \\ \mathbf{x}^T(n-1)(\mathbf{w}(n-1)-\mathbf{w}(n)) \\ \vdots \\ \mathbf{x}^T(n-\hat{M}+1)(\mathbf{w}(n-\hat{M}+1)-\mathbf{w}(n)) \end{bmatrix}. \tag{12}$$

Under the slow variation assumption of weight, i.e., $\mathbf{w}(n-i)\approx\mathbf{w}(n)$, for $i=1,\ldots,\hat{M}-1$, we see that $\hat{e}(n)\approx e(n)$. In this case, the computation of $\hat{e}(n)$ is totally avoided. Therefore, substituting $\hat{e}(n)$ with $e(n)$ in (8), together with (9), we derived our proposed new FxAPSA (NFxAPSA), which is listed in Algorithm 1. Note that if we further approximate (9) via utilizing the small step-size assumption as implementations of CFxAPA [23,26,27], we can get conventional FxAPSA (CFxAPSA) simply via $\hat{e}(n)=e(n)$ and $\hat{\mathbf{e}}_p(n-1)=\hat{\mathbf{e}}_a(n-1)$ in Eq. (8).

Please cite this article as: L. Xiao, et al., A new efficient filtered-x affine projection sign algorithm for active control of impulsive noise, Signal Processing (2015), http://dx.doi.org/10.1016/j.sigpro.2015.09.015

Algorithm 1. The NFxAPSA.

	Equation	×
1	$y(n)=\mathbf{x}^T(n)\mathbf{w}(n)$	L
2	$x_f(n)=\hat{\mathbf{s}}^T\mathbf{x}_M(n)$	$\hat{M}$
3	$\hat{\mathbf{e}}_a(n)=\begin{bmatrix} e(n) \\ \overline{\hat{\mathbf{e}}}_a(n-1)\end{bmatrix}-\mu(n-1)\begin{bmatrix} 0 \\ \overline{\mathbf{r}}_{fse}(n-1)\end{bmatrix}$	$P-1$
4	Computing $\mathbf{R}_f(n)$ via Eqs. (6) and (7)	$2P$
5	$\mathbf{r}_{fse}(n)=\mathbf{R}_f(n)\mathrm{sgn}(\hat{\mathbf{e}}_a(n))$	0
6	$\mu(n)=\dfrac{\mu}{\sqrt{\mathrm{sgn}(\hat{\mathbf{e}}_a^T(n))\mathbf{r}_{fse}(n)+\epsilon}}$	1
7	$\mathbf{w}(n+1)=\mathbf{w}(n)+\mu(n)\mathbf{X}_f(n)\mathrm{sgn}(\hat{\mathbf{e}}_a(n))$	L
	Number of multiplications: $2L+\hat{M}+3P$ (square of root: 1)	

We emphasize the difference between the proposed NFxAPSA with MFxAPSA and CFxAPSA. Instead of computing $\hat{e}(n)$ with (10) as MFxAPSA, NFxAPSA approximate it with error signal $e(n)$ according to the small step-size assumption. And NFxAPSA does not approximate the whole error vector $\hat{\mathbf{e}}_a(n)$ with both current and path error signals as CFxAPSA under this assumption, but rather computes the rest components in $\hat{\mathbf{e}}_a(n)$ recursively as in (9). In this way, we are expected approximating the performance of MFxAPSA more accurately in a large range of step-size values than CFxAPSA with similar complexity as CFxAPSA.

4. Extensions of the NFxAPSA

Two typical extensions of adaptive filtering algorithms are considered here to strengthen the effectiveness of the proposed new algorithm.

4.1. Variable step-size NFxAPSA

Variable step-size (VSS) design is an efficient technique to alleviate the conflict between fast convergence speed and low steady state misalignment of fixed case. In this part we further adapt the method in [28,18] to NFxAPSA to verify the new algorithm in the VSS case. The optimal step-size is to maximize $J(\mu)=E\|\tilde{\mathbf{w}}(n)\|_2^2-E\|\tilde{\mathbf{w}}(n+1)\|_2^2$, where $\tilde{\mathbf{w}}(n)=\mathbf{w}(n)-\mathbf{w}_o$ and $\mathbf{w}_o$ is the optimal weight. With straightforward operations, we can get an approximate optimal step-size as

$$\gamma(n)=\lambda\gamma(n-1)+(1-\lambda)\min\left(\frac{\|\hat{\mathbf{e}}_a(n-1)\|_1}{\sqrt{\beta(n-1)}},\gamma(n-1)\right), \quad (13)$$

$$\beta(n)=\mathrm{sgn}(\hat{\mathbf{e}}_a^T(n))\mathbf{r}_{fse}(n)+\epsilon. \quad (14)$$

Replacing $\mu(n)$ in Eqs. (3) and (4) with $\tilde{\mu}(n)=\gamma(n)/\sqrt{\beta(n)}$, together with the rest of NFxASPA in Algorithm 2, we get our efficient implementation of VSS-NFxAPSA. Similarly, we can also derive VSS-CFxAPSA.

4.2. Hybrid NFxAPSA

Partial update of the weight coefficients is an effective method to reduce computational complexity [29]. Instead updating coefficients partially, we update the error vector selectively. One simple strategy is

$$\hat{e}(n)=\begin{cases} e(n) & \text{If } n \text{ modulo } 2=0, \\ e(n)+\hat{\mathbf{s}}T\mathbf{y}_{\hat{M}}(n)-\mathbf{x}_f^T(n)\mathbf{w}(n) & \text{Otherwise.}\end{cases} \quad (15)$$

Substitute the above equation into (8), we can get a hybrid version of NFxAPSA (HNFxAPSA), since the update of $\hat{e}(n)$ is a hybrid of the method used in NFxAPSA and MFxAPSA. Similarly, we can also derive hybrid CFxAPSA (HCFxAPSA).

5. Complexity analysis

The computational complexity is measured by the number of multiplications and additions. The space complexity is also included in the analysis. The complexity results are summarized in Table 1 and plotted in Fig. 1 versus P with $L=192, \hat{M}=128$. From the table and figure, NFxAPSA needs as small number of multiplications $2L+\hat{M}$ as that of FxLMS, which is much smaller than the direct MFxAPSA for large projection order, without obviously sacrifice additions and space complexity.

6. Simulation results

The i.i.d. impulsive noise sequences are generated according to SαS distribution. We use the primary and secondary path data measured in [1]. The paths are modeled as finite impulsive response (FIR) with primary path length as 256, $L=192$ and $\hat{M}=M=128$, same settings as those used in [6]. The averaged noise reduction (ANR) is used as the performance evaluation criterion, with $\mathrm{ANR(dB)}=20\log_{10}(A_e(n)/A_d(n))$, where $A_e(n)=\lambda A_e(n)+(1-\lambda)|e(n)|$ and $A_d(n)=\lambda A_d(n)+(1-\lambda)|d(n)|$, $0.9\le\lambda\le 1$.

The first experiment is to compare the average ANR learning curves of the proposed algorithms with the state-of-the-art AINC algorithms, such as, FxSunLMS [3], FxlogLMS [7],

Table 1
Complexity results.

Algs.	Multiplies	Additions	Space complexity
MFxAPSA-D	$(P+3)L+2\hat{M}$	$(2P+2)L+2\hat{M}$	$(P+3)L+2\hat{M}+\max(L,\hat{M})+2P$
MFxAPSA-EEI	$3L+2\hat{M}+3P$	$(P+2)L+2\hat{M}+P^2+3P$	$(P+2)L+2\hat{M}+\max(L,\hat{M})+2P^2+6P$
MFxAPSA-EEII	$2L+5\hat{M}+5P$	$(P+1)L+(P+4)\hat{M}+P^2+4P$	$(P+3)L+(2P+6)\hat{M}+2P^2+6P$
NFxAPSA	$2L+\hat{M}+3P$	$(P+1)L+\hat{M}+P^2+3P$	$(P+2)L+\hat{M}+\max(L,\hat{M})+2P^2+6P$
CFxAPSA	$2L+\hat{M}+2P$	$(P+1)L+\hat{M}+P^2+2P$	$(P+2)L+\hat{M}+\max(L,\hat{M})+2P^2+4P$

Please cite this article as: L. Xiao, et al., A new efficient filtered-x affine projection sign algorithm for active control of impulsive noise, Signal Processing (2015), http://dx.doi.org/10.1016/j.sigpro.2015.09.015

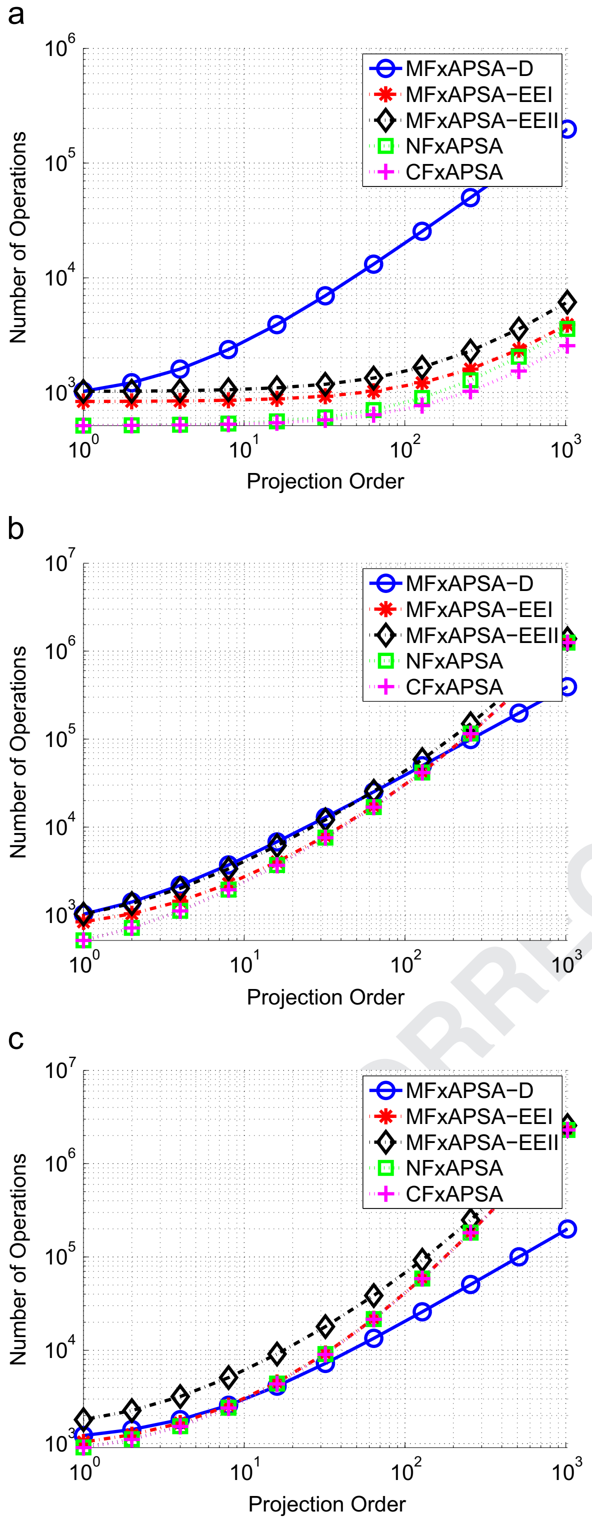

Fig. 1. Complexity results, where $L=192$, $\hat{M}=128$: (a) multiplications, (b) additions and (c) space complexity.

FwFxNLMS [9],FxGMNLMP [6] and FxMNLMM [8]. Results of the FxLMS, MFxAPSA [18] and CFxAPSA are also compared. Parameters of the related algorithms are adjusted to converge

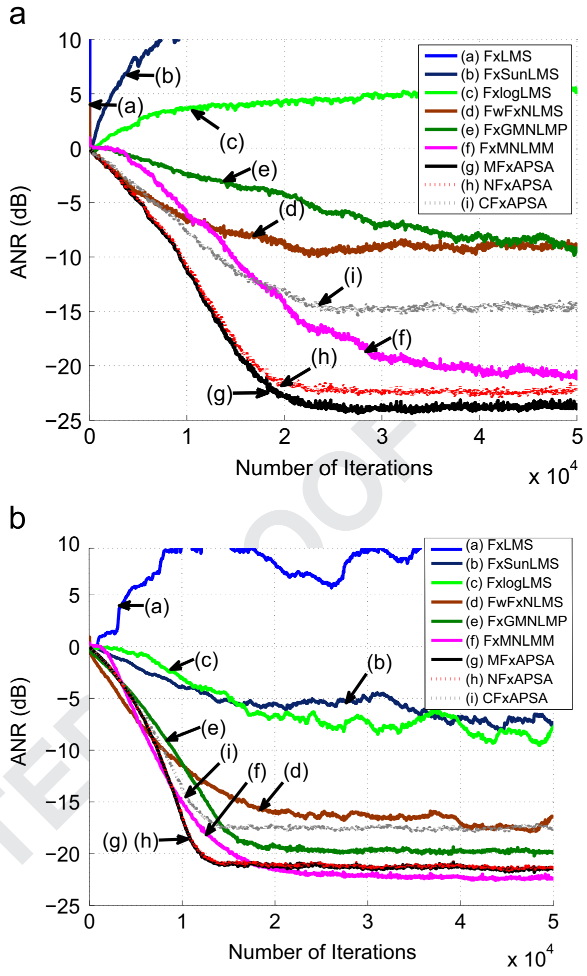

Fig. 2. The first experiment: ANR learning curves of the AINC algorithms to cancel impulsive noise according to SαS distribution. For all the versions of the MFxAPSA, $\mu=5e-4$, $P=64$: (a) $\alpha=0.6$ and (b) $\alpha=1.2$.

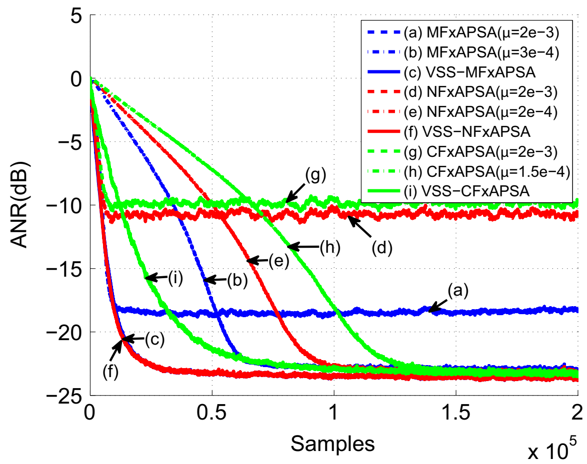

Fig. 3. The second experiment: performance of NFxAPSA versus MFxAPSA and CFxAPSA with VSS design, where inaccurate secondary path is used with SNR = 5 dB. $\alpha=1.2$, $P=8$ for fixed step-size case and $P=4$ for the VSS case. All curves are averaged over 100 independent runs.

Please cite this article as: L. Xiao, et al., A new efficient filtered-x affine projection sign algorithm for active control of impulsive noise, Signal Processing (2015), http://dx.doi.org/10.1016/j.sigpro.2015.09.015

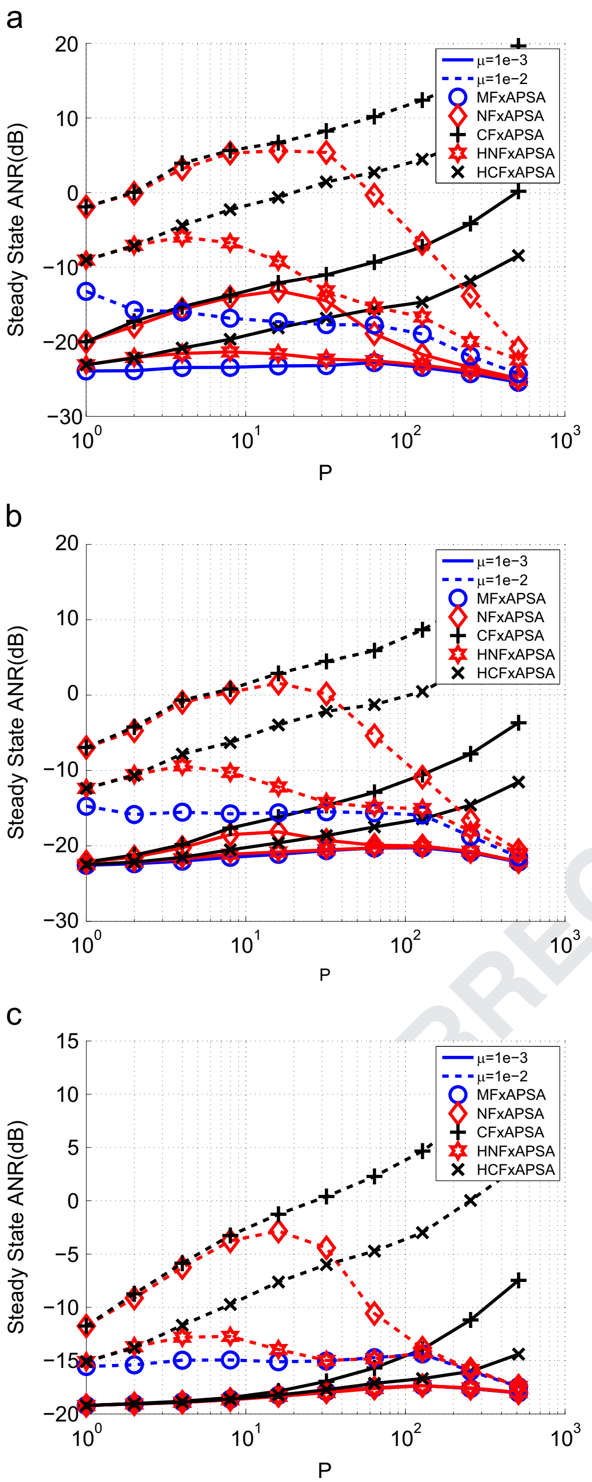

Fig. 4. The third experiment: effects of projection order on steady-state ANR performance of the MFxAPSA and its variants for canceling impulsive noises modeled as i.i.d. SαS distributions, where (a) $\alpha=0.6$, (b) $\alpha=1.2$, (c) $\alpha=2.0$. All values are averaged over 10 independent runs.

stably as fast as possible. Results in Fig. 2 show that NFxAPSA converges as fast as MFxAPSA, which outperforms all other AINC algorithms in both $\alpha=0.6$ and $\alpha=1.2$ cases.

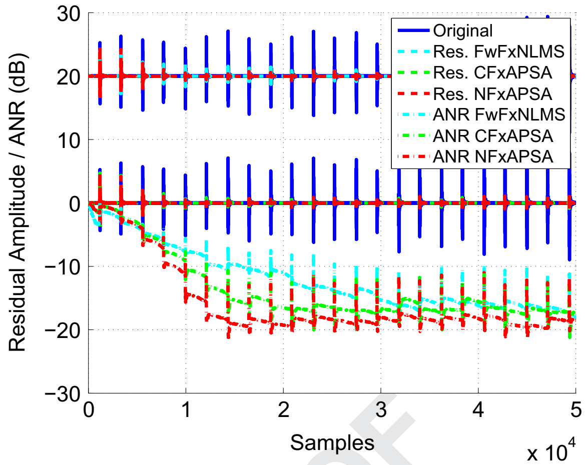

Fig. 5. The last experiment: simulation results of residual noises and ANR curves for different algorithms with pile driving noise. For NFxAPSA and CFxAPSA, $\mu=5e-4$ and $P=64$, for FwFxNLMS, $\mu=0.1$ and $\rho=0.2$.

The second experiment to demonstrate the superiorness of the new implementation is to consider the VSS case. The result is shown in Fig. 3, where $\alpha=1.2$ and the noisy estimated secondary path is used with SNR = 5 dB. With the reduced complexity, VSS-NFxAPSA is shown to have nearly the same convergence performance as VSS-MFxAPSA and to outperform VSS-CFxAPSA and others with fixed step-size design.

The third experiment is to study the influence of projection order P to the steady ANR performance of the NFxAPSA with different step-size and heaviness of impulsive noise. Results are shown in Fig. 4, where results of HNFxAPSA and HCFxAPSA are also incorporated. Interestingly, increasing the projection order P, the steady state ANR value of NFxAPSA is increasing firstly, until to some first critical point P_1, decreasing down to that of MFxAPSA after the second critical point P_2. Note that large projection order such as $P=512$ used here is to study the large projection order behavior of NFxAPSA. The HNFxAPSA has similar phenomenon, however, with some smaller first critical point, such as $P_1=4$ in all the sub-figures, where $P_1=16$ for NFxAPSA. Note that though NFxAPSA and HNFxAPSA are a little worse than MFxAPSA, yet they are more superior than both CFxASPA and HCFxAPSA, and the superiorness is more remarkable for larger projection order when $P \geq P_1$. Theoretical study of such behavior of NFxAPSA is a future work.

The last experiment is to test the performance of the NFxAPSA with the real-world impulsive noise sources, such as pile driving noise [7,9]. Both the residual waveform and the corresponding ANR curve of the NFxAPSA are plotted in the same figure in Fig. 5, where the results of FwFxNLMS and CFxAPSA are also included. From the residual waveforms, the NFxAPSA is shown to effectively cancel impulsive noise. In the steady state, NFxAPSA can reduce additional 3 dB over CFxAPSA and FwFxNLMS.

Please cite this article as: L. Xiao, et al., A new efficient filtered-x affine projection sign algorithm for active control of impulsive noise, Signal Processing (2015), http://dx.doi.org/10.1016/j.sigpro.2015.09.015

7. Conclusion

The classical FxLMS algorithm converges slowly when noise sources for ANC exhibit non-Gaussian impulsive behaviors. Via utilizing shift-structure of inputs and accurate approximating of error vector, the proposed NFxAPSA has as good performance as MFxAPSA with much reduced computational cost. The excellent AINC performance of both the standard NFxAPSA and extended ones are confirmed via simulation results with synthesized and real-world data. Theory aspect to understand the statistical behavior of NFxAPSA and applicability of the new structure to other kind of affine projection algorithms when adapted to ANC applications are two interesting issues for future works.

Acknowledgments

This research was supported by the National Natural Science Foundation of China (No. 11474306).

References

Q3

[1] S.M. Kuo, D.R. Morgan, Active Noise Control Systems: Algorithms and DSP Implementations, Wiley, 1996.
[2] R. Leahy, Z. Zhou, Y.-C. Hsu, Adaptive filtering of stable processes for active attenuation of impulsive noise, in: International Conference on Acoustics, Speech and Signal Processing (ICASSP), vol. 5, Detroit, MI, USA, 1995, pp. 2983–2986.
[3] X. Sun, S.M. Kuo, G.A. Meng, Adaptive algorithm for active control of impulsive noise, J. Sound Vib. 291 (1–2) (2006) 516–522.
[4] M.T. Akhtar, W. Mitsuhashi, Improving performance of FxLMS algorithm for active noise control of impulsive noise, J. Sound Vib. 327 (3–5) (2009) 647–656.
[5] M.T. Akhtar, W. Mitsuhashi, Improving robustness of filtered-x least mean p-power algorithm for active attenuation of standard symmetric-alpha-stable impulsive noise, Appl. Acoust. 72 (9) (2011) 688–694.
[6] M.T. Akhtar, Fractional lower order moment based adaptive algorithms for active noise control of impulsive noise sources, J. Acoust. Soc. Am. Express Lett. 132 (6) (2012) EL456–EL462.
[7] L. Wu, H. He, X. Qiu, An active impulsive noise control algorithm with logarithmic transformation, IEEE Trans. Audio Speech Lang. Process. 19 (4) (2011) 1041–1044.
[8] Y. Zou, P. Jiang, S.M. Kuo, A robust least mean m-estimate algorithm for active noise control under impulsive noise condition, in: Internoise, Osaka, Japan, 2011, pp. 1–6.
[9] L. Wu, X. Qiu, Active impulsive noise control algorithm with post adaptive filter coefficient filtering, IET Signal Process. 7 (6) (2013) 515–521.
[10] S.M. Kuo, K. Kuo, W.S. Gan, Active noise control: open problems and challenges, in: International Conference on Green Circuits and Systems (ICGCS), 2010, pp. 164–169.
[11] P.G. Georgiou, P. Tsakalides, C. Kyriakakis, Alpha-stable modeling of noise and robust time-delay estimation in the presence of impulsive noise, IEEE Trans. Multimed. 1 (1999) 291–301.
[12] M. Shao, C.L. Nikias, Signal-processing with fractional lower order moments-stable processes and their applications, Proc. IEEE 81 (7) (1993) 986–1010.
[13] P.J. Huber, E.M. Ronchetti, Robust Statistics, Wiley, 2009.
[14] A.M. Zoubir, V. Koivunen, Y. Chakhchoukh, M. Muma, Robust estimation in signal processing: a tutorial-style treatment of fundamental concepts, IEEE Signal Process. Mag. 29 (4) (2012) 61–80.
[15] T. Shao, Y.R. Zheng, J. Benesty, An affine projection sign algorithm robust against impulsive interferences, IEEE Signal Process. Lett. 17 (4) (2010) 327–330.
[16] M. Bouchard, Multichannel affine and fast affine projection algorithms for active noise control and acoustic equalization systems, IEEE Trans. Speech Audio Process. 11 (1) (2003) 54–60.
[17] A. Carini, G.L. Sicuranza, Transient and steady-state analysis of filtered-x affine projection algorithms, IEEE Trans. Signal Process. 54 (2) (2006) 665–678.
[18] L. Xiao, M. Wu, H. Sun, J. Yang, J. Tian, Modified filtered-x affine projection sign algorithm for active control of impulsive noise, in: 21st International Congress on Sound and Vibration (ICSV21), Beijing, China, 2014, pp. 1–8.
[19] J. Ni, F. Li, Efficient implementation of the affine projection sign algorithm, IEEE Signal Process. Lett. 19 (1) (2012) 24–26.
[20] F. Yang, M. Wu, J. Yang, Z. Kuang, A fast exact filtering approach to a family of affine projection-type algorithms, Signal Process. 101 (2014) 1–10.
[21] S.C. Douglas, An efficient implementation of the modified filtered-X LMS algorithm, IEEE Signal Process. Lett. 4 (10) (1997) 286–288.
[22] F. Albu, M. Bouchard, Y. Zakharov, Pseudo-affine projection algorithm's for multichannel active noise control, IEEE Trans. Audio Speech Lang. Process. 15 (3) (2007) 1044–1052.
[23] M. Ferrer, A. Gonzalez, M. Diego, G. Pinero, Fast affine projection algorithms for filtered-x multichannel active noise control, IEEE Trans. Audio Speech Lang. Process. 16 (8) (2008) 1396–1408.
[24] E. Bjarnason, Analysis of the filtered-X LMS algorithm, IEEE Trans. Speech Audio Process. 3 (6) (1995) 504–514.
[25] Y. Hinamoto, H. Sakai, Analysis of the filtered-X LMS algorithm and a related new algorithm for active control of multitonal noise, IEEE Trans. Audio Speech Lang. Process. 14 (1) (2006) 123–130.
[26] M. Ferrer, A. Gonzalez, M. Diego, G. Pinero, Transient analysis of the conventional filtered-x affine projection algorithm for active noise control, IEEE Trans. Audio Speech Lang. Process. 19 (3) (2011) 652–656.
[27] M. Ferrer, M. Diego, A. Gonzalez, G. Pinero, Steady-state mean square performance of the multichannel filtered-X affine projection algorithm, IEEE Trans. Signal Process. 60 (6) (2012) 2771–2785.
[28] J. Shin, J. Yoo, P. Park, Variable step-size affine projection sign algorithm, Electron. Lett. 48 (9) (2012) 483–485.
[29] S. Douglas, Adaptive filters employing partial updates, IEEE Trans. Circuits Syst. II: Analog Digital Signal Process. 44 (3) (1997) 209–216.

Please cite this article as: L. Xiao, et al., A new efficient filtered-x affine projection sign algorithm for active control of impulsive noise, Signal Processing (2015), http://dx.doi.org/10.1016/j.sigpro.2015.09.015